

Determination of Gamma-ray Shower Characteristics using the HEGRA Stereoscopic IACT System

A. Kohnle¹, G. Hermann^{1,2}, M. Hess^{1,3}, W. Hofmann¹, on behalf of the HEGRA collaboration

¹*MPI für Kernphysik, Postfach 103980, 69029 Heidelberg, Germany*

²*Now at Enrico Fermi Institute, University of Chicago, 933 East 56th Street, Chicago IL 60637, USA*

³*Now at SAP AG, Postfach 1461, D-69185 Walldorf, Germany*

Abstract

Characteristics of Cherenkov light emission from TeV γ -ray air showers are explored using the HEGRA system of imaging atmospheric Cherenkov telescopes. Data are presented concerning the radial distribution of Cherenkov light within the light pool, and its variation with shower energy and zenith angle, as well as on the variation of photon arrival times across the Cherenkov images.

1 Introduction

Over the last decade, imaging atmospheric Cherenkov telescopes (IACTs) have emerged as the prime instrument for the detection of cosmic γ -rays in the TeV energy regime. Both galactic and extragalactic sources of such γ -rays have been firmly established, and have been identified with pulsars, supernova remnants, and active galactic nuclei. Going beyond the existence proof for different classes of γ -ray sources, interests are increasingly turning towards precise measurements of the flux and of the energy spectra, and the search for a break or cutoff in the spectra. Such measurements require a detailed understanding of the characteristics of the Cherenkov emission from air showers, and a careful check of the simulations used to model and correct the observations. The stereoscopic observation of air showers with multiple telescopes, as pioneered in the HEGRA system of Cherenkov telescopes, allows such a detailed study of the characteristics of the Cherenkov radiation in air showers. With two telescopes, the shower geometry is fully determined. With three or more telescopes, the geometry is overdetermined and one can measure resolution functions etc. This paper summarizes results concerning the radial distribution of Cherenkov light within the light pool – a crucial input for the determination of shower energies – and on the variation of photon arrival times across Cherenkov images. A more detailed description of the analyses and the results as well as further references can be found in Aharonian et al., 1998 and Heß et al., 1998b.

The HEGRA IACT system is located on the Canary Island of La Palma, at the Observatorio del Roque de los Muchachos of the Instituto Astrofísico de Canarias, at a height of about 2200 m asl. The system comprises five identical telescopes, four of which are arranged in the corners of a square with roughly 100 m side length; the fifth telescope is located in the center of the square. The system telescopes have 8.5 m^2 mirror area, 5 m focal length, and 271-pixel cameras with a pixel size of 0.25° and a field of view of 4.3° . More details are given elsewhere in these proceedings.

The analyses presented in the following are based on the extensive sample of γ -ray events collected in observations of Mrk 501 during 1997. To determine the properties of pure γ -ray showers, the small contamination of cosmic-ray induced showers in the ‘on-source’ data samples is subtracted on a statistical basis using an equivalent ‘off-source’ region.

2 Radial distribution of Cherenkov light generated by TeV γ -ray air showers

The basic idea for this measurement is quite simple: the shower direction and core location are reconstructed based on the different views of the shower. One then selects showers of a given energy and plots the light yield observed in the telescopes as a function of the distance to the shower core. For this event selection, one should not use the standard procedures for energy reconstruction, since these procedures already assume a certain radial distribution of the light yield. Instead, a much simpler – and bias-free – method is used to select events of a

given energy: one uses a sample of events which have their core at a fixed distance d_i (typically around 100 m) from a given telescope i , and which generate a fixed amount of light a_i in this telescope. Located on a circle around telescope i , these showers cover a wide range in core distance r_j relative to some second telescope j , which in case of the HEGRA array is located between about 70 m and 140 m from telescope i . The measurement of the light yield a_j in this second telescope provides with $a_j(r_j)$ the shape of the Cherenkov light pool. Lacking an absolute energy scale, this method does provide the radial dependence, but not the absolute normalization of the light yield. To determine the distribution of light for pure γ -rays, the cosmic-ray background under the Mrk 501 signal is subtracted on a statistical basis.

For a first comparison between data and simulations, showers near the zenith (zenith angle between 10° and 15°) were selected. The range of distances r_i from the shower core to the reference telescope was restricted to the plateau region between 50 m and 120 m. Smaller distances were not used because of the large fluctuations of image size close to the shower core, and larger distances were excluded because of the relatively steep variation of light yield with distance. The showers were further selected on an amplitude in the ‘reference’ telescope i between 100 and 200 photoelectrons, corresponding to a mean energy of about 1.3 TeV. The measured radial distribution (Fig. 1(a)) exhibits a relatively flat plateau out to distances corresponding to the Cherenkov radius, and a rapid decrease in light yield for larger distances.

Shower models predict that the distribution of light intensity varies (slowly) with the shower energy and with the zenith angle. Figs. 1(a)-(c) compare the distributions obtained for different size ranges a_i of 100 to 200, 200 to 400, and 400 to 800 photoelectrons at distances between 50 m and 120 m, corresponding to mean shower energies of about 1.3, 2.5, and 4.5 TeV, respectively. We note that the intensity close to the shower core increases with increasing energy. Cherenkov light at small radii is generated by penetrating particles near the shower core. Their number grows rapidly with increasing shower energy, and correspondingly decreasing height of the shower maximum. The observed trends are well reproduced by the Monte-Carlo simulations shown as shaded bands.

The dependence on zenith angle is illustrated in Fig. 1(d)-(g), where zenith angles between 10° and 15° , 15° and 25° , 25° and 35° , and 35° and 45° are compared. Events were again selected for an image size in the ‘reference’ telescope between 100 and 200 photoelectrons, in a distance range of 50 m to 120 m¹. The corresponding mean shower energies for the four ranges in zenith angle are about 1.3 TeV, 1.5 TeV, 2 TeV, and 3 TeV. For increasing zenith angles, the distribution of Cherenkov light flattens for small radii, and the diameter of the light pool increases. Both effects are expected, since for larger zenith angles the distance between the telescope and the shower maximum grows, reducing the number of penetrating particles, and resulting in a larger Cherenkov radius. The simulations properly account for this behaviour.

3 The time structure of Cherenkov images generated by TeV γ -ray air showers

Since the HEGRA telescopes are equipped with Flash-ADC systems sampling the PMT signals at a frequency of 120 MHz, they can also be used to study the time structure of Cherenkov images.

In this context, the term ‘time structure of Cherenkov images’ is used to refer to the mean arrival time of Cherenkov photons as a function of the direction of photons, i.e., of their location within the image. Here, we concentrate on the variation of the arrival time along the major axis of the image. For each image, a coordinate system is assigned which has its origin at the image of the source, its x -axis along the major axis of the Cherenkov image, and y -axis along the minor axis of the image. The x coordinate is mainly a measure for the height h at which a photon is emitted; for a given core distance r , $x \approx r/h$.

The mean photon arrival time at a pixel at a given (x, y) will primarily vary with the direction under which showers are viewed, i.e., with the core distance r . Variations in shower energy, or image size will mainly influence the pixel amplitude, rather than its timing. Therefore, timing characteristics were studied as a function of

¹Core distance is always measured in the plane perpendicular to the shower axis

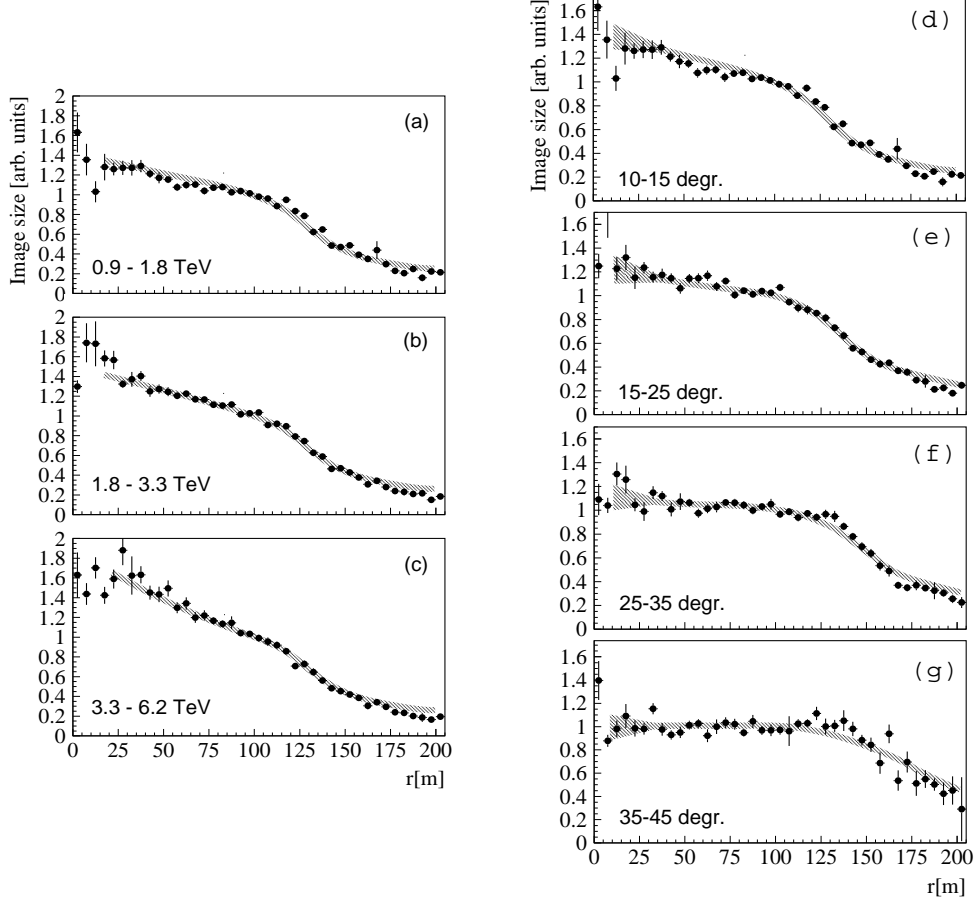


Figure 1: (a)-(c): Light yield as a function of core distance, for image *size* in the reference telescope between 100 and 200 photoelectrons (a), 200 and 400 photoelectrons (b), and 400 to 800 photoelectrons (c). The corresponding ranges in shower energy are indicated in the figure. (d)-(g) Light yield as a function of core distance, for zenith angles between 10° and 15° (d), 15° and 25° (e), 25° and 35° (f), and 35° and 45° (g). The shaded bands indicate the Monte-Carlo results. The distributions are normalized at $r \approx 100$ m. Only statistical errors are shown.

the pixel location (x, y) and of the reconstructed core distance r , averaging over a range of image *sizes* between 100 and 400 photoelectrons.

Fig. 2 shows cuts along x through the time profiles, for small $|y| < 0.1^\circ$, for γ -ray showers with different ranges in core distance. The core distance is obtained from the stereoscopic reconstruction of the showers. The profiles were obtained by sorting image pixels with $|y| < 0.1^\circ$ into bins in x according to the coordinates of the pixel centers, and averaging the arrival times in each bin over large samples of showers. The arrival time is measured relative to the average time for the whole image; negative times imply early arrival. For reference, also the intensity profiles are included, defined via the mean amplitude of pixels at a given x . As expected, the intensity profiles are asymmetric, and their width increases with increasing core distance.

Photon arrival times show a gradient along the image; at small core distances, photons at large x arrive early. For large core distances, the effect is reversed, and photons at large x arrive several ns after the bulk of the image. At intermediate distances, a roughly parabolic dependence of the arrival time on x is observed, with photons near the peak of the image arriving first. These effects are qualitatively reproduced by a simple model

(shown as full lines in the figure), which assumes that particles in the shower propagate at the (vacuum) speed of light, whereas the speed of the Cherenkov light varies according to the refractive index as a function of height. Near the shower core, light produced deep in the atmosphere (large x) arrives first, since the particle shower front propagates faster than the Cherenkov light emitted high up in the atmosphere. For large core distance, the effects of the longer path length cause light emitted deep in the atmosphere (and far from the telescope) to arrive late.

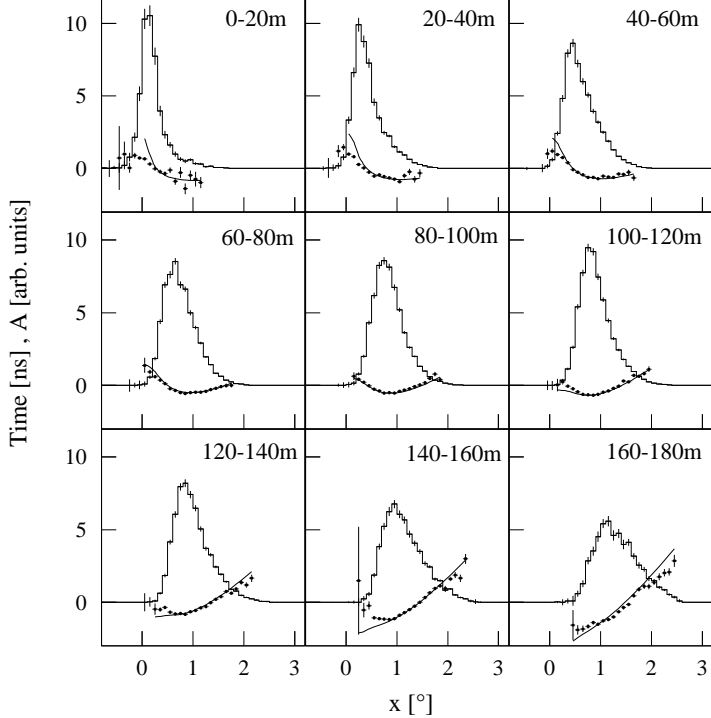


Figure 2: Longitudinal time profiles $t(x, 0)$ of γ -ray images, for different ranges in core distance (filled points). The profiles correspond to a slice along x through the image, with $|y| < 0.1^\circ$. Also shown are the corresponding intensity profiles. The smooth lines refer to the simple model for time profiles, using $v = c$ for the shower particles.

The large gradient of photon arrival time across the image, in particular at large core distances, can be used to resolve the head-tail ambiguity in the image. It also has practical implications concerning the effective integration time of PMT signals; too short integration times may truncate the head and tail of an image and result in systematic errors both in the determination of image *size* and *length*.

Of course, this brief discussion can only give a first glimpse at the wealth of data concerning shower characteristics obtained with the stereoscopic observation of air showers by multiple Cherenkov telescopes; these results will be used to improve the reconstruction of shower parameters, and to eliminate sources of systematic errors in the measurements of γ -ray energy spectra and angular distributions.

References

- Aharonian, F.A. et al., 1998, astro-ph/9807119
 Heß, M. et al., 1998, astro-ph/9812341